Scientific Journal of Impact Factor (SJIF): 4.72
e-ISSN (O): 2348-4470
p-ISSN (P): 2348-6406

International Journal of Advance Engineering and Research Development

Volume 4, Issue 11, November -2017

PHOTOLUMINESCENCE AND STRUCTURAL PROPERTY OF Ce3+ DOPED KCl SINGLE CRYSTALS

S. Bangaru[1*], S.Bharani[2]

[1*]*Associate professor of Physics, Arignar Anna Government Arts College,*
Namakkal-637002, India.
[2]*Ph.D Scholar in Physics, Arignar Anna Government Arts College,*
Namakkal-637002, India.

Abstract:- *In the present work, namely Ce^{3+} doped KCl single crystals for light emitting diode applications were grown by Bridgeman Stockbarger technique and characterized by Photoluminescence[PL], Powder X-Ray Diffraction[PXRD], Fourier Transform Infrared[FTIR], Scanning Electron Microscopy[SEM], and Vickers Microhardness[H$_V$], Electron Paramagnetic Resonance[EPR].The PL spectrum of the KCl:Ce^{3+} crystals shows a broad emission band centered at 428nm and 453nm. X-ray diffraction analysis exposed a cubic structure for the grown crystals. FTIR spectrum were used to analyze the various functional groups of the grown crystals. SEM contribute information about the surface morphology of the crystal. Mechanical strength of the grown crystals is estimated by Vicker'smicrohardness test. The work hardening co-efficient 'n' value is 2.8, this value indicates that the soft material category for the grown crystals. EPR measurements were made at X-band frequencies with 9-10 GHz field modulation at room temperature and the g-factor value are 2.3 and 2.2, calculated by using Lande's formula.*

***Keywords**: Photoluminescence, Microhardness, XRD*,SEM, EPR

1. INTRODUCTION

Nowadays much higher than average in amount to the research and development in the field of lighting technology[1].When a rare earth ions is embedded into a crystalline electron lattice interaction, some of its well localized energy states belonging to weak in the ground state 4f^{n} electronic configuration and strong in the excited state 4f^{n-1} 5d electronic configuration are located between the valence band and the conduction band of the host[2]. Lanthanide ions have a characteristic various magnetic, structural, vibrational and optical properties enabling their extensive applications studied by luminescence spectroscopy among the rare earth ions, owing to their sharp f-f (and f-d) and its application as light emitting diodes. The luminescence spectrum of Ce^{3+} ions presents in excitation and emission bands were ultraviolet and visible regions with a relatively simple energy level structure, especially the 5d(^{2}D)→^{2}F$_{j}$(j=5/2,7/2), they have been widely investigated first of all for luminescence devices, optical communications[3,4]. Among these rare earth ions, Ce^{3+} has been extensively studied because of its generally intensive, parity allowed 4f-5d transitions, otherwise one electron on the electronic configuration of the Ce^{3+} ion transitions within the 4f electronic configuration[5]. The Rare Earth ions is commonly assigned to the 4f shell. The performance of emission depends on the number of electrons in the 4f shell. Ce^{3+} ion emission has one electron in the 4f shell, which is found to be the excitation band in 4f-5d electron transitions[6,7]. Alkali halides span a wide broad band and simple structure. The possibility of incorporating dopant ion of the different sizes into alkali halide are due to their lattice parameters value varying from 7.43Å for RbI to 4.03Å for LiF[8-11]. The excellent luminescent properties for optical device applications reported on Rare earth ion doped Alkali halides[12,13]. In the present work Ce^{3+} doped KCl crystals has been grown by Bridgeman Stockbarger method and the grown crystals were characterized by vibrational, structural, magnetic, and optical properties.

2. EXPERIMENTAL DETAILS

Single crystals of Ce^{3+} doped KCl (99.99% purity) were grown using Bridgeman Stockbarger technique. Ce^{3+} was added in the form of Cerium fluoride (Aldrich; 99.99% purity). The crystals were grown in three different concentrations with impurities of 1%, 3% and 5% by weight. The studies were performed on crystals of all three concentrations. The results obtained were similar but changed in intensity in accordance with the concentration of the impurity. As a characteristics, the results obtain pertaining to the 3% concentration and are presented and analyzed. PL spectra were recorded at room temperature using a Perkin Elmer LS 55 luminescence spectrometer in the region 200-900nm with a spectral width of 5nm. The FTIR spectrum was

---

recorded using a Perkin Elmer spectrometer in the 400 – 4000cm^{-1} wave number region. The X-ray diffraction (XRD) patterns of the samples were recorded by using a CuKα radiation X-ray diffractometer. EPR spectra was recorded using a EPR spectrometer at microwave frequency at room temperature with a magnetic field modulation of 9 -10 GHz. Microhardness measurements were carried out on the cleavage planes using a Vickers' pyramidal diamond indenter. The indentations were made at different loads ranging from 25gm to 100gm for fixed azimuthal orientations of the indenter to avoid anisotropic variations. The morphologies of the KCl:Ce^{3+} crystals were revealed using a Scanning Electron Microscopy (SEM, Hitachi S-800).

3. PHOTOLUMINESCENCE

Fig.1 shows the deconvoluted excitation spectrum for Ce^{3+} doped KCl crystals were plotted by using the software ORIGIN '5.0'. The deconvoluted excitation spectrum for KCl:Ce^{3+} crystals at emission wavelength 340nm as shown in Fig.1. The excitation bands were distinguished in the middle ultraviolet wavelength region 220nm to 250nm. In this region, the intense deconvoluted excitation speaks centered at 228nm (full width half maximum 6nm) and 238nm (full width half maximum 8nm), which is assigned to the 4f-5d transition of Ce^{3+} ion.

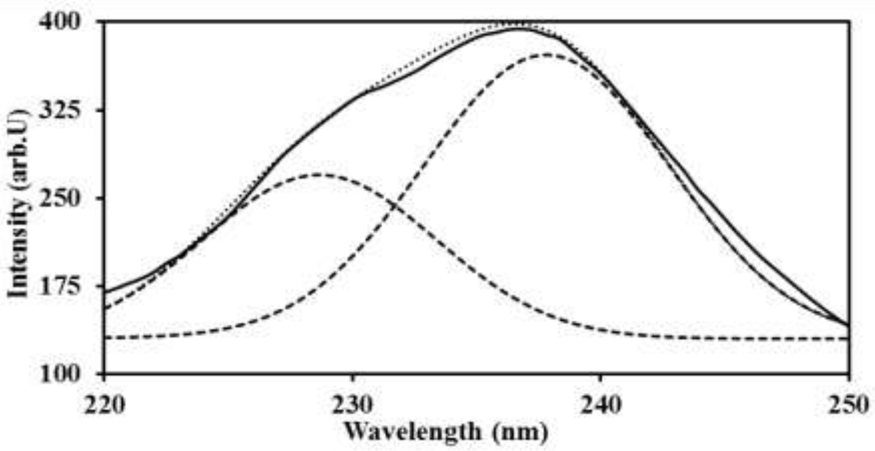

Fig.1 Excitation spectrum for Ce^{3+} doped KCl single crystals for emission at 340nm

Fig.2 shows the deconvoluted emission spectrum of the KCl:Ce^{3+} crystals were recorded at excitation wavelength of 230nm. To understand PL properties in better way, the curves were deconvoluted using the software ORIGIN '5.0'[14]. In the excitation wavelength discovered in visible region from 395nm to 500nm. Fig.2 shows that the PL emission broad bands centered at 428nm and 453nm (visible regions) are the assigned to the 5d-$^2F_{5/2}$ and 5d-$^2F_{7/2}$ transitions of Ce^{3+} ion respectively. The broad emission band of KCl:Ce^{3+} crystals could be due to an electronic transition from excited 5d→4f levels ground state of the Ce^{3+} ion[15]. The deconvoluted emission peaks have full width half maximum value of25nm and 36nm. The excitation, emission band and electron transition for KCl:Ce^{3+} crystals is summarized in table.1.

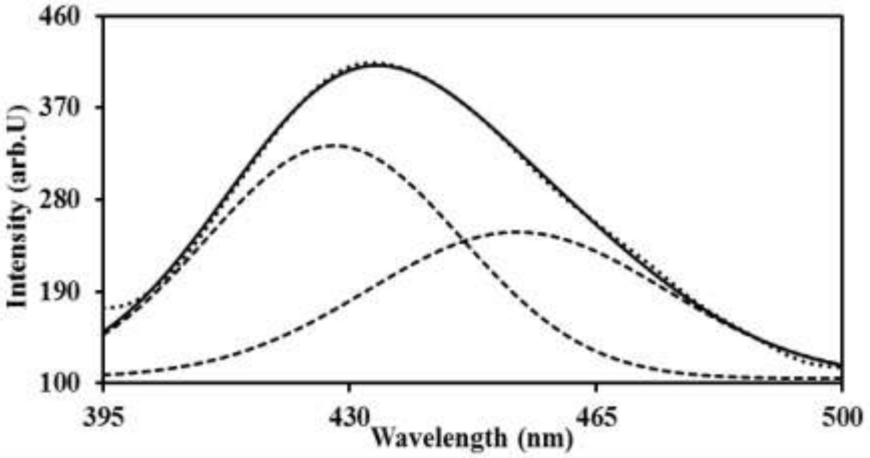

Fig.2 Emission spectrum for Ce^{3+} doped KCl single crystals for excitation at 230nm

Table.1.The excitation bands and electronic transitions for KCl:Ce^{3+} single crystals.

Sample	Types of Bands	Wavelength (nm)	Electron transition	Full Width Half Maximum (nm)
KCl:Ce^{3+}	Excitation	228	$^2F_{5/2}\rightarrow 5d$	6
		238	$^2F_{7/2}\rightarrow 5d$	8
	Emission	428	$5d(^2D)\rightarrow {}^2F_{5/2}$	25
		453	$5d(^2D)\rightarrow {}^2F_{7/2}$	36

4. POWDER X-RAY DIFFRACTION

X-Ray powder diffraction pattern of the KCl:Ce^{3+} crystals recorded by using a CuKα radiation (λ=1.5406Å). The XRD spectrum of the Ce^{3+} doped KCl crystals are shown in Fig.3. Then the hkl value of the grown crystals compared with JCPDS Card No: 75-0296 of pure KCl. The diffraction peaks are easily indexed as being consistent with the cubic structure of KCl with lattice constant a=b=c=3.14(Å), α=β=γ=90˚ and the symmetry space group is Fm3m. The cell volume is $31.2(Å)^3$. The crystallography data is given below in table.2. From Fig.3, the sharp peaks observed at 28.3 (2θ) and the calculated FWHM value are 0.001 for high intensity XRD peak (2θ~28.3). The crystallite size of KCl:Ce^{3+} crystals is evaluated using Scherrer's equation $D_c=K\lambda/\beta\cos\theta$[16-20], where D_c is average crystalline size, 'K' is the Scherrer's constant (0.94), ' λ' is the wavelength of X- ray (1.5406Å), 'β' represents full width half maxima, 'θ' is Bragg angle of the XRD peak. The broadening of the major peaks indicates the crystalline particle size, which found to be about 8.5 µm." Dislocation density" for Ce^{3+} doped KCl crystals were calculated using the equation $S=1/D^2$[21], which is found that the value are $1.3840X10^{13}$ m^{-2}.

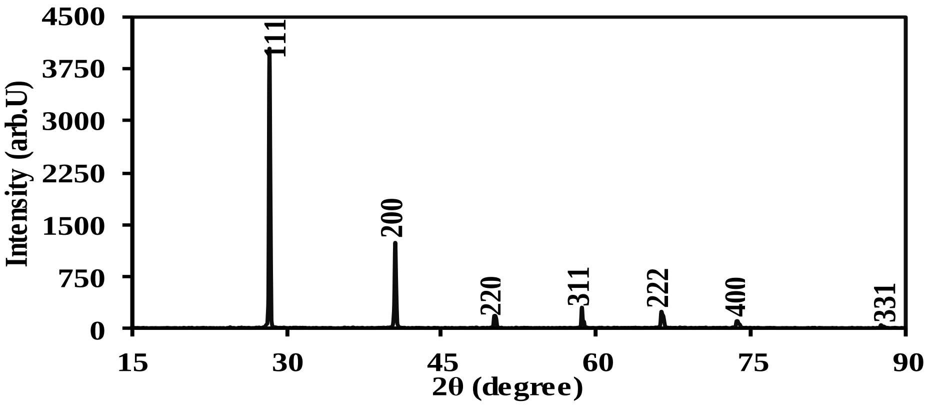

Fig.3 Powder XRD pattern of the Ce^{3+}doped KCl single crystals

Table.2. 2θ and hkl values of Ce^{3+}doped KCl single crystals.

S.No	2θ (degree)	Intensity (arb.U)	hkl values
1.	28.3	4009	111
2.	40.5	1236	200
3.	50.3	181	220
4.	58.6	301	311
5.	66.3	200	222
6.	73.7	57	400
7.	87.6	26	331

5. FOURIER TRANSFORM INFRARED

The functional groups of Ce^{3+} doped KCl crystals were identified by recording FTIR spectrum using Perkin Elmer Spectrometer in the range 400-4000 cm^{-1} which is shown in Fig.4. In FTIR spectrometer, IR radiation passes through the sample and some of the radiation are absorbed by the sample, while others are transmitted. Because of this we can measure both molecule absorption the results obtained from spectra. But here we present only transmittance spectra. The broad band at 3436cm^{-1} corresponding to O-H stretching of H_2O molecular absorbed from the atmospheric air. Hence the water molecules are elaborated in hydrogen bonding, the effective O-H force sustained within the water molecule is reduced[22-24].

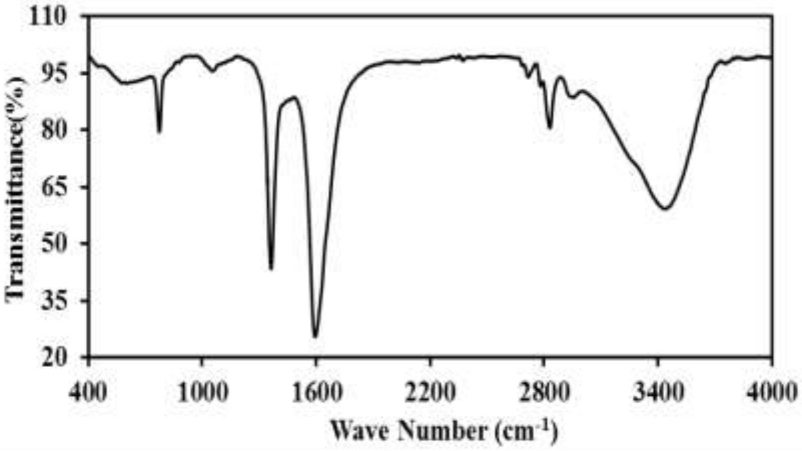

Fig.4 FTIR spectrum for Ce^{3+} doped KCl single crystals

6. SCANNING ELECTRON MICROSCOPY

Fig.5 shows the SEM micrographs of grown Ce^{3+} ion doped KCl crystals. To obtain the micrograph, the sample was coated with silver. In order to consider the surface suitability for device fabrication and also study the presence of imperfection, the Ce^{3+} doped KCl crystals were subjected to Scanning Electron Microscopy (SEM) studies. From Fig.5, it is clear that the size of the crystals is few microns to 20µm. As a result, the SEM studies declare the appearance of microcrystalline structure. At x1000 magnification the particles appear agglomerated.

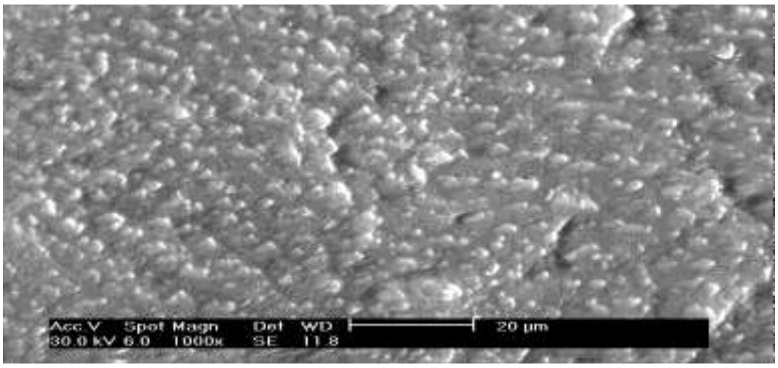

Fig.5 SEM image of Ce^{3+} doped KCl single crystals at x1000 magnification

7. VICKERS MICROHARDNESS TEST

Hardness is the resistance extent by a material, a localized plastic deformation generated by scratching or by indentations. The indentation hardness is determined as the ratio of applied load to the surface area of the indentation. The greater hardness of the metal, the greater resistance it has to deformation. Vickers hardness is a measure of the hardness of a material, calculated from the size of an impression produced under load by a pyramid shaped diamond indenter. The diagonal of the following depression is estimated by Vickers hardness number H_v is calculated using the formula $H_v=1.8544\ P/d^2\ (Kg/mm^2)$[25]. Where, P- is the applied load (measured in Kg), d- is the diagonal length of the indentation impression (measure in millimeters). Indentation were carried out using Vickers indentation for various loads 25g to 100g were shown in Fig.6. For each load, several indentations were formed and the average value of diagonal length was used to calculate the microhardness. The hardness is found to extend with load.

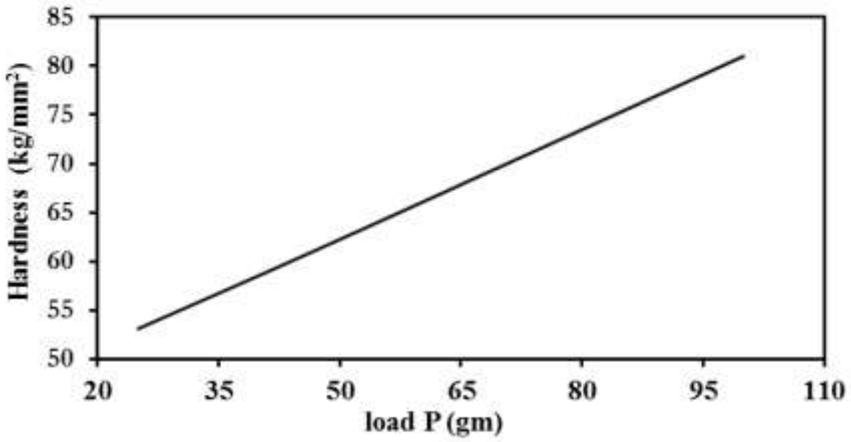

Fig.6 Variation of micro hardness number (H_v) with the applied load for Ce^{3+} doped KCl single crystals

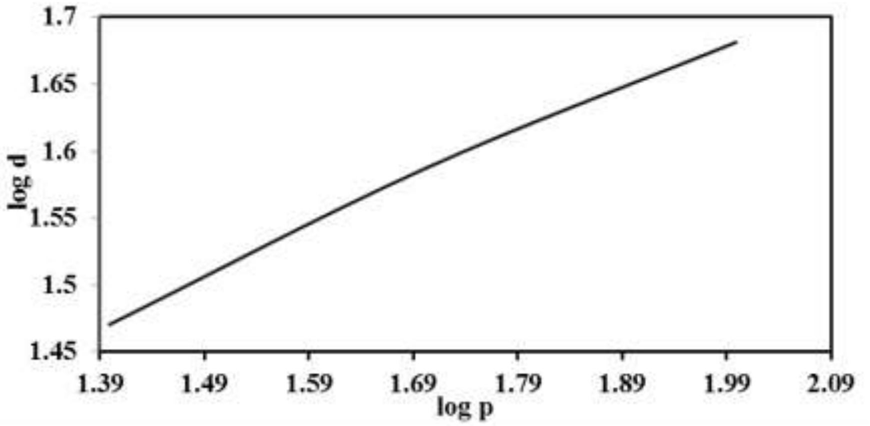

Fig.7 Plot of log P versus log d for Ce^{3+} doped KCl single crystals

The work hardening co-efficient (n) of the material is related to the load P by the relation $P=ad^n$, where 'a' is the material constant. Fig.7 shows the plotted graph of log p versus log d, which are the diagonal line. According to Onitsch[26] and Hanmann[27]the value of n should lie between 1 to 1.6 for hard materials and above 1.6 for soft materials. By plotting the graph of log P versus log d [Fig.7], the work hardening co-efficient 'n' is found to be 2.8 for Ce^{3+} doped KCl crystals, which confirms that the crystal belongs to category of soft material.

7.1 d versus $d^{n/2}$ plot

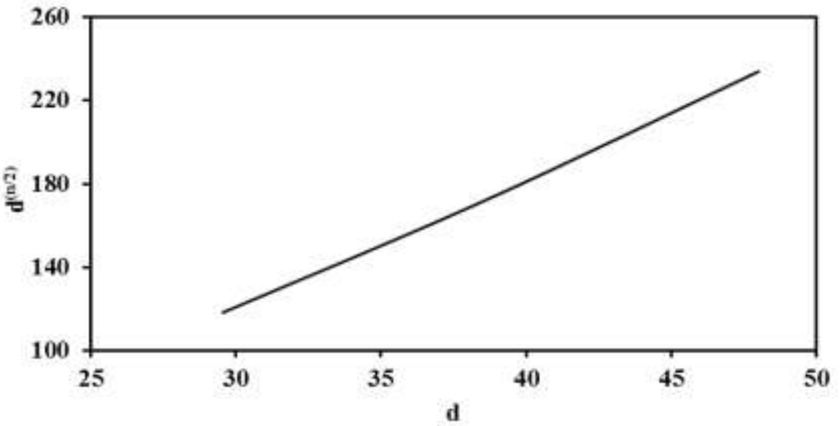

Fig. 8 d versus $d^{n/2}$ for Ce^{3+} doped KCl single crystals

It is known that the material takes some time to revert to elastic mode after the applied load is removed. The graph plotted between d Vs $d^{n/2}$ is shown in Fig.8.

7.2 Yield strength

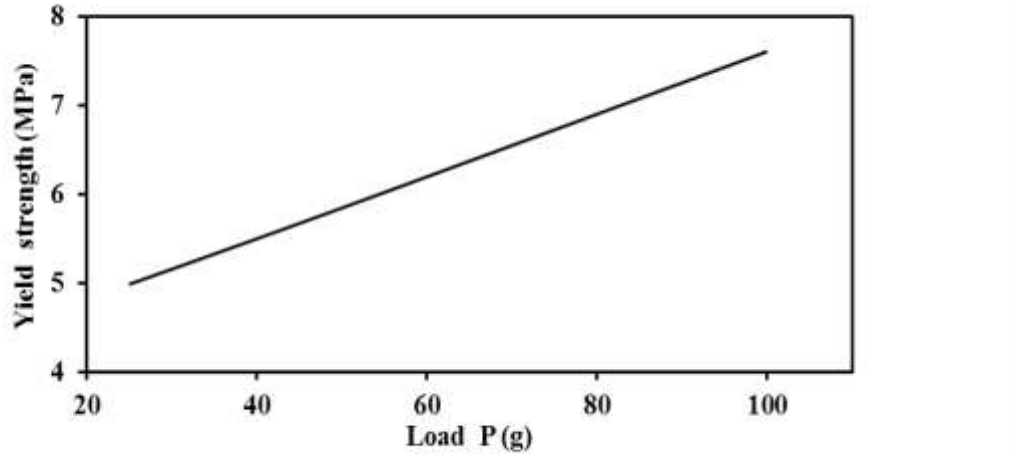

Fig.9 Dependence of yield strength with load for Ce^{3+}doped KCl singlecrystals

From the hardness value, $\sigma_y= H_v/3(0.1)^{n-2}$, this relation were used to calculate yield strength[28], where, σ_y=yield strength, H_v=hardness of the material. The yield strength is calculated to be 153.7MPa. From Fig.9, yield strength increase with increase of load and hence the grown Ce^{3+}doped KCl crystals has relatively high mechanical strength.

7.3 Elastic stiffness constant

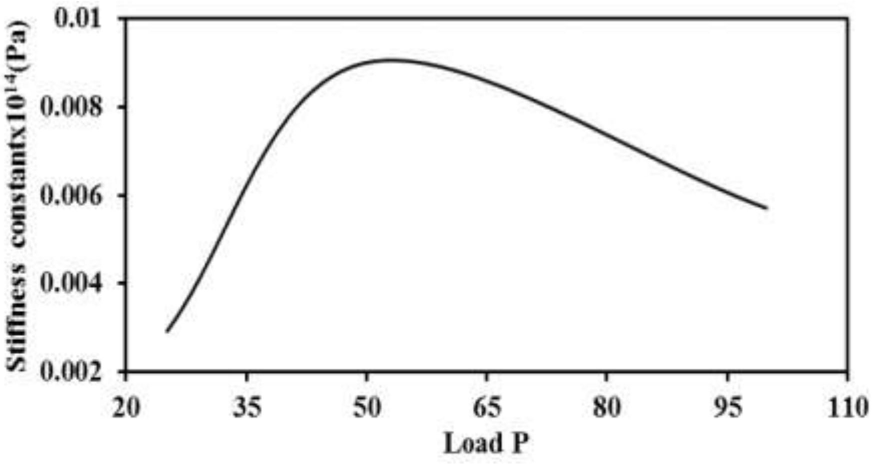

Fig.10 Plot of load P versus elastic stiffness constant for Ce^{3+}doped KClsingle crystals

The elastic stiffness constant (C_{11}) was calculated for different loads using Wooster's empirical formula $C_{11}=H_v^{7/4}$[29]. It was calculated for the loads from 25g to 100g. The plot of load P versus elastic stiffness constant for the KCl:Ce^{3+} crystals is shown in Fig.10**.** Fig 10 shows that increase of stiffness constant with increase of applied load upto 50g and after that C_{11} value decreases with applied load. This gives an indication about the tightness of bonding between neighbouring atoms upto maximum stiffness constant. The high value shows that the binding forces between the atoms were quit strong.

8. ELECTRON PARAMAGNETIC RESONANCE SPECTRUM

EPR spectrum studies were carried out at room temperature, as shown in Fig.11 for Ce^{3+} doped KCl crystals. EPR spectra were recorded using a EPR spectrometer at X-band frequency at room temperature with the magnetic field modulation of 9-10 GHz was used. The observation of resonance signals in the cubic symmetry with resonance signals depends on the zero field splitting[30-32]. The Electron Paramagnetic Resonance spectrum shows two resonance signals at 2857 Guass and 2937 Guass with an effective g value of 2.3 and 2.2 sequently. Ce^{3+} has a $4f^1$ electron configuration, as its electronic ground state ^2F_j ($j={}^2F_{5/2}$, $^2F_{7/2}$). EPR spectrum containing resonance spectral lines, which appear from the two allowed fine structure transitions for electronic spin S=1/2 (L=0) with the nucleus spin value of I=3/2 for Ce^{3+}. Ce^{3+} ion, in cubic symmetry, two resonance signals around the g factors value are g=2.3 and 2.2 to be detected. The factor has been calculated by means of using Lande's formula which is given by $g = \frac{h\nu}{\mu_B B}$,where h is the Planck's constant (6.634 x 10^{-34}), ν is the micro wave frequency, μ_B is Bohr magnetron (9.274 x 10^{-24} J/T), B is the applied magnetic field.

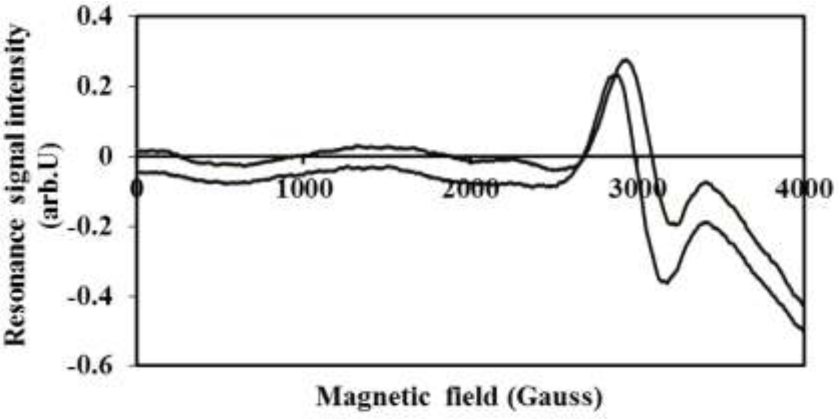

Fig.11 EPR Spectra of Ce^{3+} doped KCl single crystals

9. CONCLUSIONS

Single crystals of Ce^{3+} doped KCl crystals prepared by Bridgeman Stock Barger technique. It was found that the PL emission wavelength observed at 428nm and 453nm in KCl:Ce^{3+} crystals, which is due to 5d-4f transition of Ce^{3+} ion. This confirms that the grown crystals were suitable for LED applications. The unit cell parameters for KCl:Ce^{3+} crystals have been evaluated by X-Ray diffraction method and the structure is confirmed to be cubic system. Various functional groups present in the grown crystal have been identified by FTIR analysis. The SEM studies show the presence of microcrystalline structures ranges from few microns to 20µm. Vickers micro hardness test shows that the grown crystals fall in the category of soft material. The Yield strength of grown crystals is found to be 6.14 MPa. The EPR spectrum of the Ce^{3+}doped KCl crystals have been studied at room temperature and the g factor value is 2.3 and 2.2.

Acknowledgements

The authors great fully acknowledges the IIT, Chennai, India for providing experimental support.

References

[1]. K.Suresh, K.V.R.Murthy, N.V.Poornachandra Rao, B.Subba Rao, Synthesis and photoluminescence study of $Ca_3Si_3O_8F_2$, $Ca_5Si_2O_8F_2$ and $Ca_7Si_3O_{12}F_2$doped with Ce, Eu and Tb containing Fluorine, Inter. J. Lumin.Appli., vol.1, pp.63-66(2015).

[2]. D.Bouttet, C.Dujardin, C.Pedrini, W.Brunat, D.Tran Minh Duc, J.Y.Gesland, Proceedings of the International Conference on Inorganic Scintillators and Their Applications SCINT95, Delft University Press, The Netherlands, pp. 111,(1996).

[3]. E. Matijevic, W.P.Hsu, Preparation and properties of mono dispersed colloidal particles of lanthanide compounds, J. Colloid Inter. Sci., vol.118, pp.506-523(1987).

[4]. L.Zhu, J.Meng, X.Cao, Synthesis and photoluminescent properties of silica-coated $LaCeF_3$:Tb nanoparticles, J. Nanopart. Res., vol.10, pp.383-386(2008).

[5]. R.A.Glukhov, A.N.Belsky, C.Pedrini, A.N. Vasilev, Simulation of energy coversion and transfer in CeF_3 after VUV photo absorption, J. Alloy. Comp., vol.275, pp.488-492(1998).

[6]. K.V.R.Murthy,A.S.Saiprasad, M.R.Rao, Luminescence studies of Tb doped $YGdB_2O_6$phosphor,Phys. Proced., vol.29, pp.70-75(2012).

[7]. P.Page, R.Ghildiyal, K.V.R.Murthy, Synthesis, characterization and luminescent of $Sr_3Al_2O_6$ phosphor with trivalent rare earth dopant, Mater. Res. Bullet.,,vol.41,pp.1854-1860(2006).

[8]. V.Ausin, J.L.Alivarez Rivas, Thermoluminescence and F-Centers thermal annealing in heavily irradiated KCl and NaCl crystals, J. Phys.C: Solid Stat. Phys., vol.7, pp.2255-2262(1974).

[9]. A.A.Braner, M.Iaraeli, Effect of Illumination on the Thermoluminescence of Alkali halides, Phys. Rev., vol.132, pp.2501-2505(1963).

[10]. B.Chandra, A.R.Lakshmanan, R.C.Bhatt, Effect of Deep Traps on the Sensitation in LiF (TLD-100) Phpsphor, Phys. Stat.Solid.A,vol.60, pp. 593-598 (1980).

[11]. G.T.Hageseth, Optical Absorbtion and Thermoluminescence of X-Ray Irradiated KBr Crystals at Room Temperature, Phys.Rev.B, vol.5, pp.4060-4064(1972).

[12]. O.Gorodetskaya, R.Reisfeld, O.K.Jorgensen, Proceeding of the international, congress on glass, Bolet.De LaSocied.Espan. De Ceram. Y Vidrio,vol.31, pp.472-479(1992).

[13]. C. Vijayan, Y.V.G.S. Murti, Thermoluminescence of KCl:Gd^{2+} containing, Z$_1$-centres, Cryst.Latt. Defect. Amorp.Mater.,vol.18, pp.431-439(1989).

[14]. T.Ding, W.T.Zheng, H.W.Tian, J.F.Zang, Z.D.Zhao, S.S.Yu et al, Temperature-dependent photoluminescence in La2/3Ca1/3MnO3, Solid Stat.Commun.,vol.132, pp.815-819(2004).

[15]. L.Bian, F.Du, S.Yang, Q.Ren, Q.L.Liu, Crytsal structure and Near – ultraviolet photoluminescence properties of $Ba_9Sc_2Si_6O_{24}$:Ce^{3+},Na^{+}, J. Lumin., vol.137, pp.168-172(2013).

[16]. R.Sankar, G.V.Subba Rao,Eu^{3+} luminescence, Ce^{4+}→Eu^{3+} energy transfer and White-Red light generation in Sr_2CeO_4, J. Electrochem. Soc., vol.147, pp.2773-2779(2000).

[17]. Y.D.Jiang, F.Zhang, C.J.Summers, Synthesis and properties of Sr_2CeO_4 blue emission powder phosphor for field emission displays, Appl. Phys.Lett.,vol.74, pp.1677-1679(1999).

[18]. O.A.Serra, V.P.Severino, P.S.Calefi, S.A.Cicillini, The blue phosphor Sr_2CeO_4 synthesized by pechini's method, J. Alloy. Comp.,vol.667, pp. 323–324(2001).

[19]. Y.B.Khollam, S.B.Deshpande, P.K.Khanna, P.A.Joy, H.S.Potdar, Microwave accelerated hydrothermal synthesis of blue white phosphor:Sr2CeO4, Mater. Lett.,vol.58, pp. 2521-2524(2004).

[20]. Y.K.Tang, H.P.Guo, Q.Z.Qin,Photoluminescence of Sr_2CeO_4 phosphors prepared by microwave calcination and pulsed laser deposition, Solid Stat.Commun., vol.121, pp.351-356(2002).

[21]. G.Santhi, M.Alagar, Growth and characterization of single crytsals of thiourea and tartaric acid based compounds, Imperial J. Interdisip. Res., vol.2, pp.537-541(2016).

[22]. G.Kaur, S.K. Singh and S.B.Rai, Eu^{3+} and Yb^{3+}codoped Gd_2O_3 single phase nanophosphor: An enhanced monochromatic red emission through coparativeupconversion and downconversion, J. Appl. Phys.,vol.107, pp.073514-1-073514-6(2010).

[23]. J. Chandradass, M. Balasubramanian, D.S.Bae and H.Kim, Materials and Manufacturing Processes, 27 J.W. Lee, J. Korean Ceram. Soc.,vol.47, pp.177-182(2010).

[24]. T.Selvalakshmi, S. Sellaiyan, A. Uedono, A. Bose, investigation of defect related photoluminescence property of multicolor lighting Gd_2O_3:Dy^{3+} phosphor, RSCAdvan.,vol.4, pp. 34257-34266(2014).

[25]. S.Sivananthan, N.Neelakanda Pillai, N.N.Pillai, C.K.Mahadevan, Hardness measurements on pure and ZnS added $NaCl_x$ Br_{1-x} single crystals grown from aqueous solutions, Archive. Phys. Res.,vol.3239-244(2012).

[26]. E.M.Onitsch, Aboutthemicrohardness of metals, Mikroskopie,vol.2, pp.131-151(1947).

[27]. M.Hannman, Indentation size effectandmicrohardness study, Metal. Manch,vol.23, pp. 135-139(1941).

[28]. R.Jothi Mani, P.Selvarajan, Growth, Hardness Parameters, Laser Damage Threshold and Thermal Analysis of L-Alanine Crystals Grown in Aqueous Solution of Hydrofluoric Acid (LAHF), Inter. J. Innovat. Res. Sci. Eng.,vol.2, pp.612-615(2014).

[29]. W.A.Wooster, Physical Properties and atomic arrangements in crystals, Report. Prog. Phys., vol.1662-82(1953).

[30]. K.Kawano, M.Shimizu,R.Nakata, M.Sumita, EPR study on a cubic ^{151}Eu^{2+} and a pseudo cubic (^{151}Eu^{2+}, Sr^{2+}) in alkali halides, Radiat. Effect.,vol.73, pp.167-172(1983).

[31]. A.Edgar, J.Zimmermann, H.Von seggern, C.R.Varoy, Lanthanum-stabilized europium-doped cubic barium chloride: an efficient x-ray phosphor, J. Appl.Phys., vol.107, pp.083516-1 - 083516-7(2010).

[32]. H.Vrielinck, D.G.Zverev, P.Leblans, J.P.Tahon, P.Matthys, F.Callens, Electron Paramagnetic Resonance Study Of Eu^{2+} Centers In Melt-Grown CsBr Single Crystals, Phys.Rev.B, vol.85, pp.144119-1 – 144119-7(2012).